ELSEVIER

Solid State Ionics 135 (2000) 71–79

SOLID STATE IONICS

www.elsevier.com/locate/ssi

Effect of iron on the electrochemical behaviour of lithium nickelate: from $LiNiO_2$ to 2D-$LiFeO_2$

C. Delmas[a,*], G. Prado[a], A. Rougier[a], E. Suard[b], L. Fournès[a]

[a]*Institut de Chimie de la Matière Condensée de Bordeaux ICMCB-CNRS and ENSCP de Bordeaux, Av. Dr Schweitzer, 33608 Pessac, Cedex France*

[b]*Institut Laue Langevin, BP 166X, 38042 Grenoble, Cedex France*

Abstract

Iron substituted lithium nickelate have been obtained by high temperature solid state chemistry. The general formula deduced from structural analysis is $Li_{1-z}(Ni_{1-y}Fe_y)_{1+z}O_2$. Layered phases are obtained for $y \leq 0.30$. The Rietveld refinements of the X-ray diffraction patterns show that, in normal synthesis conditions, the amount of 3d cations in the lithium plane ranges between 0.06 and 0.08. The neutron diffraction study of a material which contains a large amount of extra-cations ($z = 0.14$) shows that there is no lithium ions in the nickel plane; i.e. there is no cationic mixing. The comparative Mössbauer study of lithium phases with homologous strict 2D sodium phases shows that a small amount of iron ions is in the lithium plane in good agreement with the result previously reported by Reimers and Dahn [1]. The electrochemical behaviour of these materials has been studied in lithium batteries. The reversible capacity is small vs. unsubstituted phases. A Mössbauer spectroscopy study has shown that iron and nickel are simultaneously oxidised upon lithium deintercalation. The electrochemical behaviour of these materials has been compared to that of layered $LiFeO_2$ and $NaFeO_2$.

Keywords: Intercalation; Layered oxides; Lithium batteries; Mössbauer spectroscopy; Lithium nickelate; Iron oxides

1. Introduction

With the aim of finding new positive electrode materials for lithium-ion batteries, a very strong research and development effort has been devoted to the study of $LiNiO_2$ which exhibits two main advantages vs. $LiCoO_2$: its lower cost and a higher reversible capacity. Nevertheless, its higher instability in the oxidised state and the capacity fading upon cycling require an improvement of this material by cationic substitution if practical applications are expected. Presently, some lithium nickel oxide derivatives are considered by the battery producers to be very promising for application in 4 V lithium-ion batteries.

In the frame of our general studies on layered oxides and in particular on $LiNiO_2$ derivatives, an investigation of iron substitution has been undertaken. The $LiNi_{1-y}Fe_yO_2$ system was first studied by Dahn and coworkers [1]. These authors found that a single phase, isostructural to $LiNiO_2$, could be obtained in the $0 \leq y \leq 0.23$ range and that the iron

*Corresponding author. Tel.: +33-5-56-846296; fax: +33-5-56-846634.

E-mail address: delmas@icmcb.u-bordeaux.fr (C. Delmas).

0167-2738/00/$ – see front matter
PII: S0167-2738(00)00333-7

substitution led to a decrease in the electrochemical activity. Preliminary studies performed in our lab globally confirmed those results [2]. By chimie douce reactions from sodium layered oxides, Fuchs and Kemmler-Sack prepared for the first time layered $LiFeO_2$ [3]. A systematic study of this material and of the $LiNi_{1-y}Fe_yO_2$ solid solution was performed by Kanno and co-workers [4–6]. In the case of the pure iron phase, numerous studies were reported mainly by Tabuchi's research group [7,8]; a very poor electrochemical behaviour was found.

The iron substituted phases are interesting from the fundamental point of view since Mössbauer spectroscopy is a very sensitive characterisation tool to investigate the local structure and electronic configuration. In two very recent papers, we reported on the detailed characterisation of the structure and the electrochemical properties of the $LiNi_{1-y}Fe_yO_2$ phases, respectively [9,10]. In this more general one, we give an overview of their properties in order to clarify the behaviour of iron ions in layered oxides.

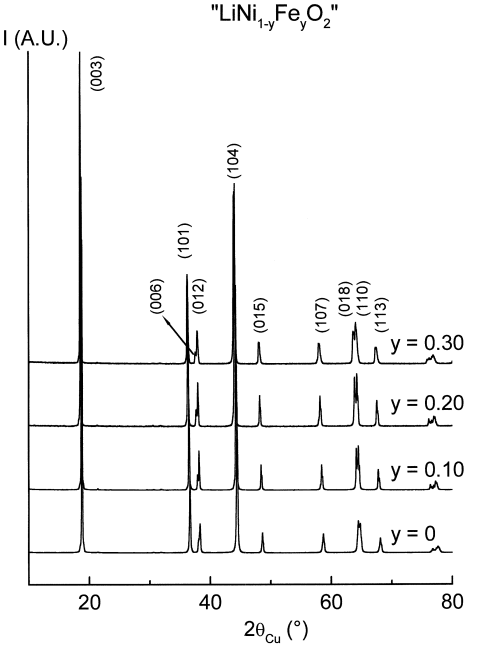

Fig. 1. X-ray diffraction patterns of layered $LiNi_{1-y}Fe_yO_2$ phases.

2. Results and discussion

The various materials were prepared either by direct synthesis from the oxides or through the precipitation of a precursor phase in order to improve the homogeneity. In the first way, the Li_2CO_3, NiO and Fe_2O_3 mixture is fired for 10 h at 600°C and then for 48 h at 800°C under oxygen. In the second way, an iron and nickel nitrate solution is precipitated by an $LiOH + NH_4OH$ solution [11]. After drying under vacuum at 90°C and then in an oven for 15 h at 110°C, the precursor phase is fired for 5 h at 750°C under oxygen. Generally the $Li/Ni + Fe$ ratio used for the synthesis was equal to 1, but in some cases, in order to obtain materials with a large amount of 3d cations in the lithium site, lower values of this ratio were used. Characterisation of the materials by XRD, Mössbauer spectroscopy and electrochemistry does not give evidence of any significant difference between the materials obtained by the two techniques.

The XRD analysis shows that a layered type phase of general formula $LiNi_{1-y}Fe_yO_2$ is obtained for $0 \leq y \leq 0.30$. For higher y values, the limit phase is mixed with a cubic one which is obtained alone for $y > 0.50$. All these results agree with the earlier ones obtained by Reimers et al. [1]. The only difference is in the upper limit of the solid solution which is slightly higher in our case, which must result from slight differences in the synthesis conditions. As shown in Fig. 1 which gives the XRD patterns of the pure layered phases, the materials are very well crystallised; the splitting of the (018) and (110) diffraction lines emphasises the 2D character of the structure.

3. Structural characterisation

3.1. X-ray and neutron diffraction

The structure of all the layered materials was determined by Rietveld analysis. These materials crystallise in the α-$NaFeO_2$ type structure (*R-3 m* space group). The hexagonal cell parameters are given in Table 1. As in unsubstituted lithium nickelate, a significant departure from stoichiometry was evidenced; the formula of the material deduced from the X-ray diffraction analysis is $Li_{1-z}(Ni_{1-y}Fe_y)_{1+z}O_2$ in good agreement with the

Table 1
Hexagonal cell parameters and amount of 3d cations (z) in the interslab space of $Li_{1-z}(Ni_{1-y}Fe_y)_{1+z}O_2$ phases

y	0.1	0.2	0.2	0.3
$a_{hex.}$ (Å)	2.8903(1)	2.8955(1)	2.9003(1)	2.9008(1)
$c_{hex.}$ (Å)	14.2607(7)	14.3017(9)	14.3142(11)	14.3417(15)
z	0.061(3)	0.084(7)	0.145(5)	0.074(5)

chemical analyses. The amount of cations (nickel or iron) in the lithium site (z) is also reported in Table 1. These z values are significantly larger than those obtained in similar synthesis conditions for the unsubstituted lithium nickelate ($z_{Ni} = 0.02$) [12]. As previously mentioned in this latter reference, while X-ray diffraction is very sensitive to the presence of the 3d element in the lithium site, it is quite insensitive to the presence of lithium in the nickel site of lithium nickelate; therefore, a small cationic mixing (Li^+/Ni^{3+} exchange) cannot be deduced from the Rietveld analysis of XRD patterns. A convenient way to determine if there is a cationic mixing is to use neutron diffraction. Such a study has been performed on a $Li_{1-z}(Ni_{0.8}Fe_{0.2})_{1+z}O_2$ phase where a strong lithium deficiency was voluntary introduced in order to increase the probability to have a cationic mixing. This experiment was carried out on the D2B diffractometer of the Institut Laue–Langevin in Grenoble. The results of the Rietveld refinement of the neutron diffraction pattern are identical to those obtained by XRD and there is no evidence of the presence of lithium in the nickel site. The amount of nickel or iron in the lithium site ($z = 0.14$) is also identical to that found from XRD.

In the $Li_{1-z}Ni_{1+z}O_2$ system, the presence of z extra-nickel ions requires the existence of 2 z Ni^{2+} which are equally distributed between the $[NiO_2]$ slabs and the interslab spaces. As confirmed by the Mössbauer study presented in the following, in the case of iron substituted phases, divalent iron ions are not expected in the presence of trivalent nickel. Therefore, the extra-cations in the lithium sites must be either divalent nickel or possibly trivalent iron. The difference in ionic radii ($r_{Ni^{2+}} = 0.69$ Å, $r_{Fe^{3+}} = 0.645$ Å, $r_{Li^+} = 0.76$ Å [13]) shows that both 3d cations can occupy the lithium sites even if Ni^{2+} ions are slightly favoured. The very close atomic diffusion factors of nickel and iron cannot allow, in classical diffraction experiments, to discriminate between these two cations. Using anomalous X-ray scattering, Reimers et al. have shown that both cations are in the lithium site [1]. This is quite important from the electrochemical point of view, since the irreversible loss at the first cycle, which, in the $Li_{1-z}Ni_{1+z}O_2$ system, has been related to a local collapse of the structure when the extra-nickel ions are oxidised to the trivalent state [14] must be affected by the nature of the cations in the lithium site. The difference in ionic radii and in redox potentials of nickel and iron ions involved during the electrochemical process must also play an important role.

3.2. Evidence of extra-cation from magnetic and Mössbauer characterisation

As reported in numerous papers, the magnetic properties of lithium nickelate are very sensitive to the stoichiometry of the material [12,15–18]. The presence of divalent extra-nickel ions in the lithium plane leads to the formation of ferrimagnetic clusters statistically distributed within the structure. Depending on their concentration and their distribution within the crystallites, the macroscopic magnetic properties can change from a paramagnetic behaviour (or a superparamagnetic one) to a ferrimagnetic one [19].

The thermal variations of the reciprocal magnetic susceptibility (χ^{-1}) of the $LiNi_{1-y}Fe_yO_2$ phases are shown in Fig. 2. The shape of the curves obtained in this study, where only the low temperature range has been explored, is very similar to that found for the $Li_{1-z}Ni_{1+z}O_2$ phases [12,16]. In the latter system, the study of the magnetic properties in an extended temperature range clearly emphasises the ferrimagnetic behaviour. Comparison of the curves of the iron-substituted samples to that of the $Li_{0.98}Ni_{1.02}O_2$ phase clearly shows that there is a significant amount of ferrimagnetic clusters around the extra-3d cations of the lithium site. For the three materials, the Curie temperature, which is directly related to the amount of clusters, is close to 100 K. This result is in agreement with the presence of very similar amounts of $Ni^{2+}(Fe^{3+})$ ions in the lithium site.

In order to confirm the existence of this magnetic transition, a comparative Mössbauer spectroscopy

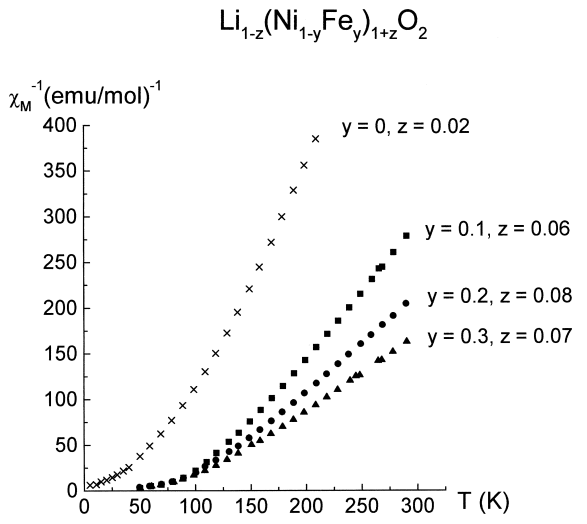

Fig. 2. Thermal variation of the reciprocal magnetic susceptibility of layered $Li_{1-z}(Ni_{1-y}Fe_y)_{1+z}O_2$ phases.

study was realised on all materials at room temperature and at 4.2 K. The results obtained in the case of the $Li_{1-z}(Ni_{0.8}Fe_{0.2})_{1+z}O_2$ ($z = 0.08$) phase are reported in Fig. 3. At room temperature, the Mössbauer spectrum is characteristic of high spin trivalent iron ions in octahedral site in a paramagnetic phase, while the appearance of six lines at low temperature shows the existence of a magnetically ordered phase. It should be mentioned that a paramagnetic line remains at low temperature; it results from superparamagnetic properties which can be attributed to the non homogeneous distribution of the clusters within the structure: the magnetic properties are very sensitive to the cluster percolation [19]. The detailed structural characterisation by Mössbauer spectroscopy is reported in the next section.

3.3. Mössbauer spectroscopy

It was shown in the previous sections that a significant amount of nickel and/or iron ions are in the lithium site. In order to try to distinguish between both cations, a systematic study of these materials by Mössbauer spectroscopy was performed. This study was extended to homologous layered sodium phases ($NaFeO_2$ and $NaNi_{1-y}Fe_yO_2$) which present a strictly 2D structure [20], i.e. with no 3d cation in the sodium layer. Fig. 4 shows the Mössbauer spectra

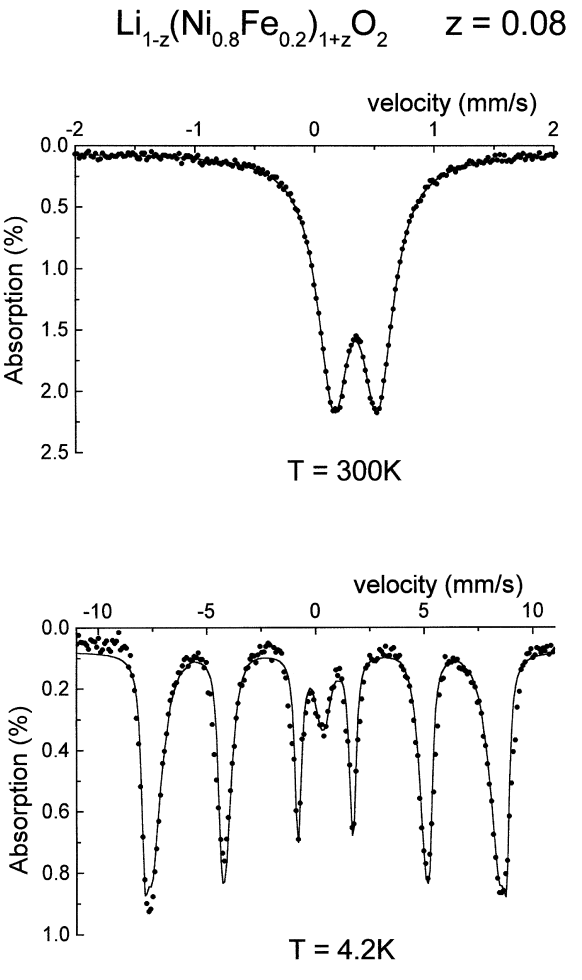

Fig. 3. Mössbauer spectra of the $Li_{0.92}(Ni_{0.8}Fe_{0.2})_{1.08}O_2$ phases at room temperature and at 4.2 K.

obtained at room temperature for three materials ($Li_{1-z}(Ni_{0.8}Fe_{0.2})_{1+z}O_2$ $z = 0.08$, $z = 0.14$ and $NaNi_{0.6}Fe_{0.4}O_2$). These typical results are given as examples but the study was performed on numerous compositions in the lithium and in the sodium systems. All materials exhibit isomer shifts (IS) which vary in the 0.33–0.35 mm s^{-1} range and average quadrupolar splittings ($\overline{QS}$) which vary between 0.33 and 0.50 mm s^{-1}. The values of the isomer shift are characteristic, as expected, of high spin trivalent iron ions in octahedral sites. The quadrupolar splitting increases in the lithium phases with the amount of substituting cations. This indicates that the average asymmetry of the iron environ-

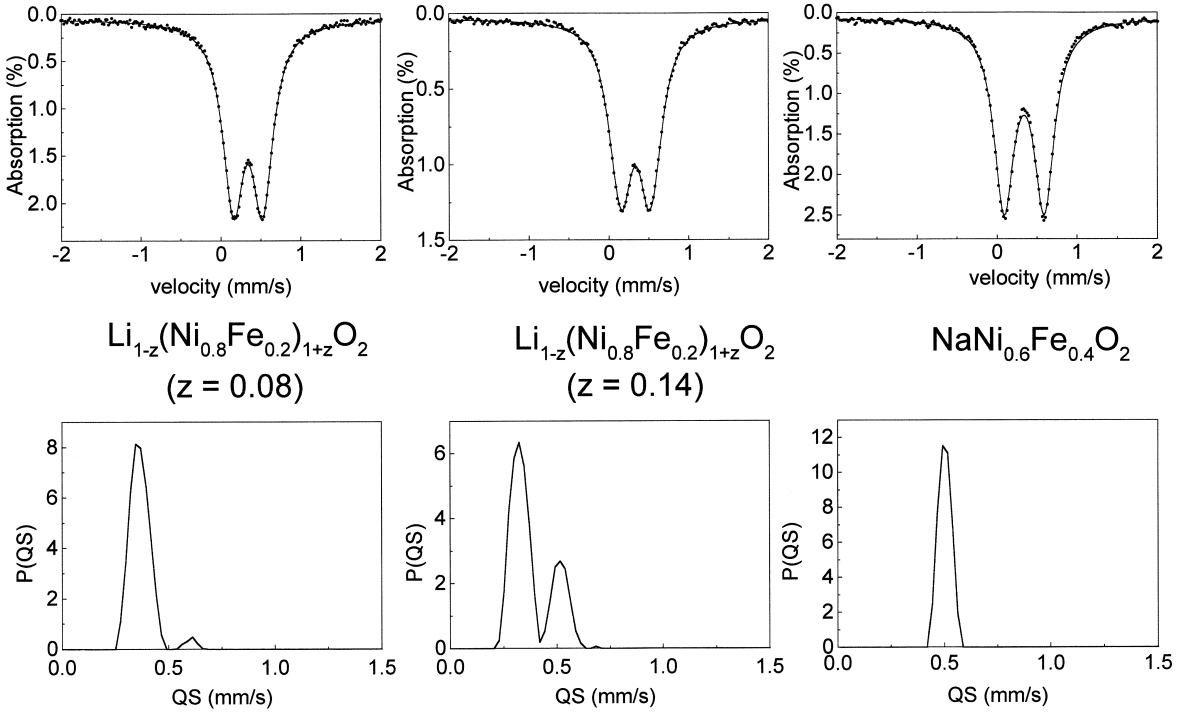

Fig. 4. Mössbauer spectra and distribution of the quadrupolar splittings of $Li_{1-z}(Ni_{1-y}Fe_y)_{1+z}O_2$ and $Na(Ni_{0.6}Fe_{0.4})O_2$ phases at room temperature.

ment increases when iron is substituted for nickel. Moreover, the linewidth also increases with the amount of iron which suggests the existence of a distribution of quadrupolar splittings and therefore of local iron environments. In order to get more insight about this point, the Mössbauer spectra were fitted by considering a distribution of quadrupolar splittings with a constant value of the linewidth (0.30 mm s^{-1}). The distribution of the quadrupolar splitting, given in Fig. 4, clearly shows the existence of discrete environments for iron ions. Clearly, for the sodium phase which presents a strictly layered structure, there is only one type of environment from the Mössbauer point of view. This shows that the difference in surrounding due to the distribution of Ni^{3+} and Fe^{3+} within the slabs is too small to be detected by Mössbauer spectroscopy. Comparison of the quadrupolar distribution for the two phases with 20% of iron but different amount of 3d cations (z_{3d}) in the lithium site suggests that the second set of quadrupolar splittings observed for the high QS values is due to the presence of iron in the interslab space. Nevertheless, since, when z_{3d} increases, the amount of Ni^{2+} ions also increases, one has to consider the effect of these ions on the quadrupolar splitting. In fact, their presence in the vicinity of an [FeO_6] octahedron could lead to a high value of the quadrupolar splitting. Comparison of the area of the peaks associated to each distribution to the amount of divalent nickel statistically present in the vicinity of an iron ion shows unambiguously that the second set of quadrupolar splittings is not related to the presence of divalent nickel ions.

Therefore, in conclusion of this section, one can consider that a part of the substituting iron cations are in the lithium site in good agreement with the results obtained by Reimers et al. from anomalous scattering experiments [1].

4. Electrochemical behaviour

All these materials mixed with carbon and PTFE in the 88:10:2 ratio were used as positive electrode

of lithium batteries with a 1 M solution of $LiPF_6$ in PC/EC/DMC as electrolyte. These batteries were cycled galvanostatically or potentiostatically under various conditions. Fig. 5 shows the cycling curves obtained from the materials with 10 and 20% of iron which contain 6% and 8% of extra-Ni(Fe) ions in the lithium sites, respectively. In both cases, the deintercalation/intercalation process is completely reversible. The capacity loss at the first cycle is large for the $y=0.1$ phase and very large for the $y=0.2$ one. The cell polarisation and the slope of the *V(x)* curve in the second part of the charge increase rapidly with *y*, which contributes in reducing significantly the reversible capacity.

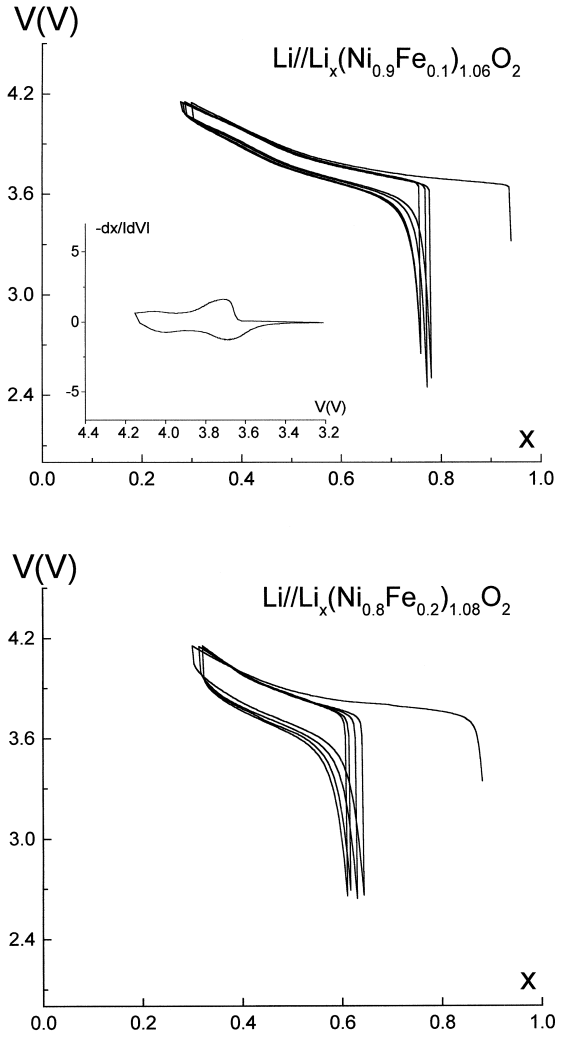

Fig. 5. Electrochemical cycling curve of $Li_{1-z}(Ni_{1-y}Fe_y)_{1+z}O_2$ phases $y=0.1$, $z=0.06$ and $y=0.2$, $z=0.08$. For the first one the derivative is given in inset. ($I=315$ μA; 23 mg of material).

The shape of the cycling curve is quite monotonous and does not exhibit plateaux as clearly shown by the variation of $-dx/|dV|$ vs. *V* curve (Fig. 5). This suggests the existence of a solid solution in the whole deintercalation domain. This was confirmed by an XRD study of partially deintercalated materials. All these phases are isotypic with the non-deintercalated ones. The variation of the hexagonal cell parameters with the amount of lithium *x* corresponds to the one observed classically in layered oxides: a decrease of $a_{hex.}$ due to the cation oxidation and an increase of the c_{hex}. parameter due to oxygen–oxygen electrostatic repulsions through the interslab space when lithium ions are removed. In the case of the Li_xNiO_2 system, all the plateaux which appear on the cycling curves have been related to lithium/vacancy ordering as clearly shown by electron diffraction experiments [21,22]. In the case of substituted materials when the amount of substitution is high enough, the cationic disordering within the slab prevents a lithium/vacancy ordering within the interslab space and an overall solid solution is observed in the whole composition domain during the cycling [23].

A Rietveld refinement of the X-ray diffraction pattern was realised for the composition $Li_{0.53}(Ni_{0.9}Fe_{0.1})_{1+z}O_2$. In this experiment, the cell was built up from $Li_{0.92}(Ni_{0.9}Fe_{0.1})_{1.08}O_2$ as positive electrode material. Generally, on materials removed from the electrochemical cell, the refinement is quite difficult and cannot be completed. In this case, it was successful and all parameters including the atomic displacement factors were correctly fitted. Two main results arise from this fit: there is no change in the amount of cations in the interslab space ($z=0.08$) and the average Ni(Fe)–O distance has significantly decreased upon oxidation [1.951 Å vs. 1.984 Å in the starting material]. This variation is very similar to that found in the $Li_{1-z}Ni_{1+z}O_2$ system [24]. This decrease in the metal–oxygen distance agrees quite well with the ionic radii of nickel and oxygen ions ($r_{Ni^{3+}}=0.56$ Å, $r_{Ni^{4+}}=0.48$ Å, $r_{O^{2-}}=1.40$ Å). Nevertheless, one must consider the effect of these

very small distances on the iron oxidation state. In order to try to clarify this point a Mössbauer study has been performed on deintercalated phases.

4.1. Mössbauer characterisation of the deintercalated materials

Several deintercalated phases with $Li_x(Ni_{0.9}Fe_{0.1})_{1.06}O_2$ composition were prepared electrochemically in the $0.28 \leq x \leq 0.94$ range. These materials were characterised by Mössbauer spectroscopy at room temperature as shown in Fig. 6. Several features appear readily: (i) appearance of new absorption lines corresponding to low values of the isomer shift which means that iron ions have been partially oxidised, (ii) increase of the quadrupolar splitting which means that the symmetry of the environment has decreased, (iii) increase in the linewidth which suggests the existence of a distribution in the iron environments. The fit of these patterns shows the presence of three types of iron ions (trivalent iron, tetravalent iron and average oxidation state '$Fe^{3.5+}$') [25,26]. This latter species corresponds formally to an electron exchange between adjacent iron ions. In fact, the behaviour can be much more complicated if more than two iron cations are in neighbouring octahedra. In all cases, the iron ions are in highly distorted octahedral sites with the high spin configuration. The fit also allows the relative concentration of each type of ions to be determined for each deintercalation amount (Fig. 7a).

Oxidation of iron seems quite surprising; moreover, one must remember that in the similar cobalt-substituted phases, trivalent cobalt ions are oxidised

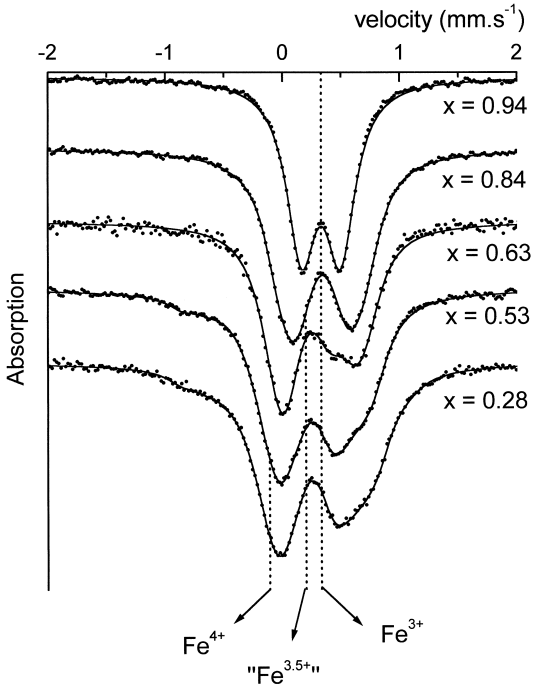

Fig. 6. Mössbauer spectra of the deintercalated $Li_x(Ni_{0.9}Fe_{0.1})_{1.06}O_2$ phases at room temperature.

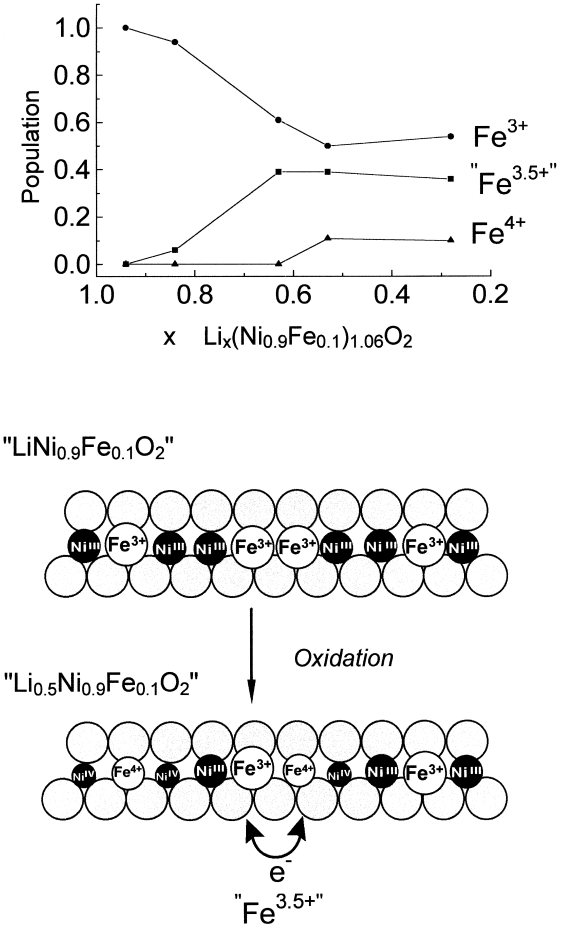

Fig. 7. Variation with x of the various iron populations and schematic distribution of the cationic oxidation states upon lithium deintercalation.

only when all nickel ions have been oxidised to the tetravalent state [23,27]. This general behaviour can be explained by the modifications in the ligand field around the substituting cation imposed by the prevailing nickel ions. In these layered structures, within the slabs the octahedra share edges; therefore, the cation–anion distance around each type of cation is mainly fixed by the overall structure and not only by the intrinsic size of the involved cation [28]. In the case of cobalt substitution, the Co^{3+} ions are smaller than the Ni^{3+} ones; therefore, upon oxidation there is no tendency to reduce the Co–O distance before the Ni–O one: nickel ions are oxidised in a first step. The opposite behaviour is observed in the case of the iron substituted system. Due to the large size of Fe^{3+} ions, these ions are compressed in their octahedra, there is a strong tendency to reduce the iron–oxygen distance upon deintercalation and a partial oxidation of iron occurs.

As schematically illustrated in Fig. 7b, several situations can occur depending on the iron distribution at the local scale. Completely isolated iron ions surrounded by Ni^{4+} ions are oxidised to the tetravalent state. When two iron ions are in neighbouring octahedra, the oxidation leads to an intermediate oxidation state due to an electron exchange. When several cations are close to one another or in the vicinity of an interslab cation, where there is an excess of positive charge one can assume that iron ions remain at the trivalent state. A very similar behaviour has been observed several years ago in iron-substituted nickel oxyhydroxide with related layered structures [25,29,30].

Due to the presence of 0.06 (Ni^{2+}/Fe^{3+}) ions in the interslab spaces 0.12 Ni^{2+} are present in the starting material. As previously discussed in the case of the Li_xNiO_2 system [31], one can assume that upon lithium deintercalation those of the slabs are oxidised in a first step, while there is competition between the oxidation of those of the interslab spaces and the oxidation of nickel to the tetravalent state within the slabs due to the difference in size of the octahedra. This behaviour can explain why the oxidation of iron is not observed at the beginning of the oxidation. Moreover, due to the large size of the octahedra in the lithium layer, one can reasonably assume that the iron ions which are in these sites remain at the trivalent state.

5. General discussion

From the results discussed above, it is interesting to consider the behaviour of iron in layered oxides from a general point of view.

As previously mentioned, lithium deintercalation from layered $LiFeO_2$ is very difficult. In this case, the iron–oxygen distance is fixed by the ionic radius of iron; therefore, the [FeO_6] octahedra are not compressed like in the iron-substituted lithium nickelate and the iron oxidation is not facilitated. One can assume that a significant lithium deintercalation from this phase could occur, but at a higher voltage, out of the electrochemical stability window of the electrolyte.

In the same purpose, it is interesting to consider sodium deintercalation from α-$NaFeO_2$ which has been reported 15 years ago by Kikkawa et al. [32] and more recently by Yamamoto's and Takeda's research group [20]. The first authors, using bromine as oxidising agent obtained the $Na_{0.9}FeO_2$ composition, while the second ones reached $Na_{0.5}FeO_2$ by electrochemical oxidation. As expected from the chemical formula, their Mössbauer studies showed that iron is oxidised to the tetravalent state. The cell voltage vs. lithium metal required to deintercalate sodium was 3.7 V. We have shown in previous studies that in general the difference in cell voltage between Li//$LiMO_2$ and Na//$NaMO_2$ cells is close to 1 V [33]. In this voltage difference, 0.3 V comes from the negative electrode while the remaining 0.7 V results from the difference in lattice energy between the sodium and the lithium phase. If one extrapolates this result to the layered $LiFeO_2$ phase, a 4.4 V cell potential would be required to deintercalate this material.

All these studies show the very strong effect of the structure and of the ligand field imposed by the prevailing cations on the redox properties of the 3d element. Investigations in this field are a promising way to tailor the electrochemical properties of intercalation compounds.

Acknowledgements

The authors wish to thank ILL for the neutron diffraction facilities and Région Aquitaine and CNES for financial support.

References

[1] J.N. Reimers, E. Rossen, C.D. Jones, J.R. Dahn, Solid State Ionics 61 (1993) 335.
[2] A. Rougier, Thesis, University of Bordeaux I, France, 1995.
[3] B. Fuchs, S. Kemmler-Sack, Solid State Ionics 68 (1994) 279.
[4] R. Kanno, T. Shirane, Y. Inaba, Y. Kawamoto, J. Power Sources 68 (1997) 145.
[5] K. Ado, M. Tabuchi, H. Kobayashi, H. Kageyama, O. Nakamura, Y. Inaba, R. Kanno, M. Takagi, Y. Takeda, J. Electrochem. Soc. 144 (1997) L177.
[6] T. Shirane, R. Kanno, Y. Kawamoto, Y. Takeda, M. Takano, T. Kamiyama, F. Izumi, Solid State Ionics 79 (1995) 227.
[7] M. Tabuchi, C. Masquelier, T. Takeuchi, K. Ado, I. Matsubara, T. Shirane, R. Kanno, S. Tsutsui, S. Nasu, H. Sakaebe, O. Nakamura, Solid State Ionics 90 (1996) 129.
[8] M. Tabuchi, K. Ado, H. Kobayashi, I. Matsubara, H. Kageyama, M. Wakita, S. Tsutsui, S. Nasu, Y. Takeda, C. Masquelier, A. Hirano, R. Kanno, J. Solid State Chem. 141 (1998) 554.
[9] G. Prado, E. Suard, L. Fournès, C. Delmas, J. Mater. Chem. (submitted)
[10] G. Prado, A. Rougier, L. Fournès, P. Willmann, C. Delmas, J. Electrochem. Soc. (submitted)
[11] D. Caurant, N. Baffier, B. Garcia, J.P. Pereira-Ramos, Solid State Ionics 91 (1996) 45.
[12] A. Rougier, P. Gravereau, C. Delmas, J. Electrochem. Soc. 143 (1996) 1168.
[13] R.D. Shannon, C.T. Prewitt, Acta Cryst. B25 (1969) 925.
[14] C. Delmas, J.P. Pérès, A. Rougier, A. Demourgues, F. Weill, A. Chadwick, M. Broussely, F. Perton, P. Biensan, P. Willmann, J. Power Sources 68 (1997) 120.
[15] J.B. Goodenough, D.G. Wickahm, W.J. Croft, J. Appl. Phys. 29 (1958) 382.
[16] A. Hirano, R. Kanno, Y. Kawamoto, Y. Takeda, K. Yamaura, M. Takano, K. Ohyama, M. Ohashi, Y. Yamaguchi, Solid State Ionics 78 (1995) 123.
[17] A. Rougier, C. Delmas, G. Chouteau, J. Phys. Chem. Solids 57 (1996) 1101.
[18] A.L. Barra, G. Chouteau, A. Stepanov, A. Rougier, C. Delmas, European Physical Journal B 7 (1999) 551.
[19] D. Mertz, Y. Ksari, F. Celestini, J.M. Debierre, A. Stepanov, C. Delmas, Phys. Rev. B (in press)
[20] Y. Takeda, K. Nakahara, M. Nishijima, N. Imanishi, O. Yamamoto, M. Takano, R. Kanno, Mat. Res. Bull. 29 (1994) 659.
[21] J.P. Pérès, F. Weill, C. Delmas, Solid State Ionics 116 (1999) 19.
[22] C. Delmas, M. Ménétrier, L. Croguennec, S. Levasseur, J.P. Pérès, C. Pouillerie, G. Prado, L. Fournès, F. Weill, J. Inorg. Mat. 1 (1999) 11.
[23] I. Saadoune, C. Delmas, J. Solid State Chem. 136 (1998) 8.
[24] J.P. Pérès, A. Demourgues, C. Delmas, Solid State Ionics 111 (1998) 135.
[25] L. Guerlou-Demourgues, L. Fournès, C. Delmas, J. Electrochem. Soc. 143 (1996) 3083.
[26] Y. Fournès, Y. Potin, J.C. Grenier, G. Demazeau, M. Pouchard, Solid State Comm. 64 (1987) 239.
[27] I. Saadoune, M. Ménétrier, C. Delmas, J. Mater. Chem. 7 (1997) 2505.
[28] C. Delmas, M. Ménétrier, L. Croguennec, I. Saadoune, A. Rougier, C. Pouillerie, G. Prado, M. Grüne, L. Fournès, Electrochimica Acta (in press).
[29] L. Demourgues-Guerlou, L. Fournès, C. Delmas, J. Solid State Chem. 114 (1995) 6.
[30] P. Axmann, C.F. Erdbrügger, O. Glemser, Angew. Chemie 35 (1996) 1115.
[31] J.P. Pérès, C. Delmas, A. Rougier, M. Broussely, F. Perton, P. Biensan, P. Willmann, J. Phys. Chem. Solids 57 (1996) 1057.
[32] S. Kikkawa, S. Miyazaki, M. Koizumi, Mat. Res. Bull. 20 (1985) 373.
[33] C. Delmas, in: G.A. Nazri, J.M. Tarascon, M. Armand (Eds.), Materials Research Society Symposium, Solid State Ionics III, Vol. 293, 1993, p. 15, Boston, USA.